J. Fluid Mech. (1972), *vol.* 56, *part* 1, *pp.* 1–18
Printed in Great Britain

Conditionally sampled measurements near the outer edge of a turbulent boundary layer

By R. A. ANTONIA
Department of Mechanical Engineering, The University of Sydney

(Received 4 May 1972)

The conditional sampling technique is used to measure ensemble averages of the longitudinal and normal velocity fluctuations u and v respectively and of the Reynolds shear stress fluctuations uv both within the turbulent and irrotational regions near the outer edge of a turbulent boundary layer. The measurements are made in both a smooth- and a rough-wall boundary layer under zero-pressure-gradient conditions. The smooth- and rough-wall results are qualitatively similar but the magnitude of the rough-wall averages is higher than that of the smooth-wall averages, corresponding with the higher value of wall shear stress on the rough surface. The maximum shear stress value encountered within a burst represents a significant proportion of the wall shear stress.

The statistical properties of the turbulence within the burst are close but not quite identical to the nearly Gaussian properties of the inner region of the boundary layer. During an attempt to distinguish between bursts of different ages or strengths at the time of measurement, it was found that bursts of relatively short duration travel at much the same longitudinal velocity as the local mean U and contribute little to the local shear stress. The longer and less frequent bursts have a mean velocity smaller than U and a maximum shear stress comparable to the shear stress at the wall.

1. Introduction

The large-scale motion which is directly responsible for the shape and entrainment properties of the turbulent–irrotational interface of the turbulent boundary layer and various other free turbulent shear flows has recently been experimentally studied by means of the conditional sampling and averaging technique (Kovasznay, Kibens & Blackwelder 1970; Imaki 1968; Kaplan & Laufer 1969; Wygnanski & Fiedler 1970). Unlike measurements of conventional averages which give equal weight to the contributions from the turbulent and non-turbulent regions, in the conditional sampling technique the flow property of interest is sampled and averaged only during that part of the time when the flow is either turbulent or irrotational. In the investigation of turbulent boundary layers, the conditional or selective sampling technique has also been used when examining some of the features of the small-scale motion associated with the 'bursts'† or

† The large-scale bursts or bulges in the intermittent outer region of the boundary layer are the subject of the present investigation. To avoid confusion, inverted commas are used whenever reference is made to the smaller scale bursts which have been observed by Kline *et al.* (1967) and others near the viscous sublayer.

eruptions observed by Kline *et al.* (1967) in the immediate vicinity of a smooth wall. The conditional measurement idea has also been used by Wygnanski (1971) in the investigation of turbulent slugs in the transitional pipe-flow regime and would generally be useful for the study of turbulent flows with superposed periodicity.

Although fairly systematic measurements of conditional averages in intermittently turbulent flows have appeared only recently in the literature, it should be noted that the concept has been known for some time. Townsend (1949, 1956) reported measurements of the longitudinal and normal velocity averaged in the outer turbulent region of the wake whilst Rotta (1956) estimated the laminar and turbulent mean velocity profiles from strip chart records of the output from a hot wire placed in the transitional flow region of a pipe. In the work of Kim, Kline & Reynolds (1968), the hydrogen-bubble time-marker method was used to obtain a quantitative idea of the Reynolds shear stress and turbulent energy production only during periods of time which correspond to the 'bursts' or eruptions mentioned above.

In the present paper, the notion of an ensemble average is used to gain some understanding of the large-scale structure of turbulence near the outer edge of a turbulent boundary layer. The ensemble average is obtained by first sampling the flow quantity of interest at various values of t/T, where t is the time measured from the beginning of either a burst or an irrotational patch of flow between two consecutive bursts and T is the duration of that particular burst or irrotational patch. The averaging is next performed over a number of bursts or irrotational regions. Ensemble averages of the longitudinal and normal velocity fluctuations u and v, respectively, and of the Reynolds shear stress fluctuation uv are obtained near $y/\delta = 1{\cdot}0$ (δ being the boundary-layer thickness and y the distance from the wall) for approximately self-preserving boundary layers developing on both smooth and rough walls. The rough-wall boundary layer chosen has a turbulence structure in the inner region of the flow which is significantly different (Antonia & Luxton 1971*a*) from that in the corresponding region of the smooth wall.

2. Experimental technique

2.1. *Experimental conditions*

The measurements presented in §§4 and 5 were obtained at only one position very near the edge of both smooth- and rough-wall zero-pressure-gradient boundary layers which were very closely self-preserving. The free-stream velocity U_1 was approximately 18 ft/s for both the smooth- and rough-wall conditions and the Reynolds number $U_1\theta/\nu$ (θ being the momentum-layer thickness) was 2160 for the smooth wall and 4030 for the rough wall. The smooth-wall measurements were made at $y/\delta = 0{\cdot}947$, where the intermittency factor γ (the fraction of time for which the flow is turbulent) was 0·19, and the rough-wall measurements were for $y/\delta = 1{\cdot}0$, where $\gamma \simeq 0{\cdot}14$. Some of the boundary-layer parameters are given in table 1. The k-type roughness used consisted of rectangular slats of $\frac{1}{8}$ in. square cross-section. These slats spanned the width of the working section at a

	Smooth wall	Rough wall
y/δ	0·947	1·0
δ (in.)	1·90	2·80
θ (in.)	0·23	0·43
U_1 (ft/s)	18·28	18·28
$C_f\ (=\tau_w/\frac{1}{2}U_1^2)$	0·0036	0·0084
$\overline{(u^2)}^{\frac{1}{2}}/U_\tau$	0·465	0·361
$\overline{(v^2)}^{\frac{1}{2}}/U_\tau$	0·395	0·306
$-\overline{uv}/\tau_w$	0·060	0·030
γ	0·187	0·137
$\overline{u}_t/U_\tau$	−0·365	−0·456
$\overline{(u-\overline{u}_t)_t^2}/\tau_w$	0·728	0·470
$\overline{u}_p/U_\tau$	0·082	0·086
$\overline{(u-\overline{u}_p)_p^2}/\tau_w$	0·073	0·047
$\overline{v}_t/U_\tau$	0·205	0·284
$\overline{(v-\overline{v}_t)_t^2}/\tau_w$	0·493	0·316
$\overline{v}_p/U_\tau$	−0·045	−0·042
$\overline{(v-\overline{v}_p)_p^2}/\tau_w$	0·068	0·041
$(\overline{(uv)_t}-\overline{uv})/\tau_w$	−0·112	−0·240
$(\overline{(uv)_p}-\overline{uv})/\tau_w$	0·030	0·034
F_u†	9·82	12·01
F_v	7·82	11·93
F_{uv}	96·6	127·0
$F_{\langle u_t\rangle}$	2·79	4·32
$F_{\langle u_p\rangle}$	4·64	3·66
$F_{\langle v_t\rangle}$	2·88	4·27
$F_{\langle v_p\rangle}$	4·23	3·78
$F_{\langle (uv)_t\rangle}$	17·54	18·40
$F_{\langle (uv)_p\rangle}$	5·58	9·26
$U_1\overline{T}_t/\delta$	0·269	0·216
$U_1\overline{T}_p/\delta$	1·300	1·490
$U_1\overline{T}_{tot}/\delta$	1·692	1·860

† F_u is the flatness factor of the whole signal but $F_{\langle u_t\rangle}$ is the flatness factor of only the turbulent signal, relative to its respective ensemble average, i.e.

$$F_{\langle v_t\rangle} = \langle (u-\langle u_t\rangle)_t^4\rangle / (\langle (u-\langle u_t\rangle)_t^2\rangle)^2.$$

TABLE 1. Boundary-layer characteristics and statistical properties of signals at measuring stations

pitch of $\frac{1}{2}$ in. More details about the wind-tunnel configuration and the geometry of the rough surface may be found in Antonia & Luxton (1971*a*).

All measurements were made with a Disa X-probe (type 55A38). The 5 μm diameter Pt-plated tungsten wires were operated with a non-linearized constant-temperature anemometer designed by Fraser (1969). The signals from the anemometer were recorded in digital form after passing through accurately matched 1 kHz sharp cut-off filters. The sampling frequency was set at 3000 samples per second. This frequency was set after examination of power spectra, which show little significant energy above 1 kHz. The digital records were processed on the English Electric KDF 9 computer in the University of Sydney. Several programs were developed for obtaining both conventional and conditional averages. For

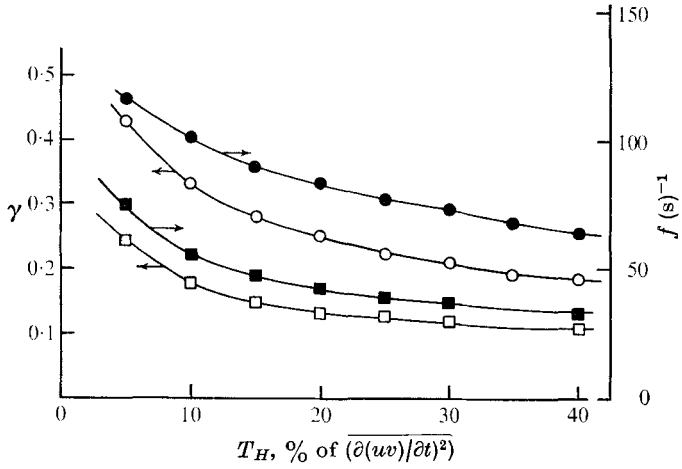

FIGURE 1. Variations of f and γ with threshold setting T_H. Smooth wall: ○, γ; ●, f. Rough wall: □, γ; ■, f.

most of the results presented here, the length of record analysed was $16\frac{2}{3}$ s but in a few cases records of up to 30 s duration were used. The $16\frac{2}{3}$ s record was found to be sufficient to obtain stationary values of both conventional and conditional averages.

2.2. *Generation of criterion function*

Before the conditional averages could be obtained the intermittency function $I(t)$, defined by $I = 1$ in the turbulent fluid and $I = 0$ in the non-turbulent fluid, needed to be set up. An examination of the instantaneous u and v signals, the longitudinal and normal velocity fluctuations respectively, and of uv, the fluctuating Reynolds shear stress, clearly indicated that for this relatively low Reynolds number flow uv would be much more suitable than either u or v for detecting the turbulent–irrotational interface. Considerable fluctuations of u and v are found in the non-turbulent parts of the flow whilst the uv signals (see figure 2) shows virtually no fluctuations in the irrotational regions with the result that the effective signal-to-noise ratio for uv is significantly larger than that for either u or v. *A posteriori* quantitative verification of this may be found in § 5.

The criterion adopted for determining $I(t)$ was that $(\partial(uv)/\partial t)^2$ had to exceed a certain threshold value over a suitably small 'hold' time. The threshold parameter was arbitrarily set at a small percentage of $(\partial(uv)/\partial t)^2$ averaged over the complete record. The need for the hold or delay time arises from the observation that $(\partial(uv)/\partial t)^2$ can, on occasions, momentarily exceed or drop below the threshold value. Ideally this delay time would need to be of the order of the Kolmogoroff length scale divided by some suitable convection velocity of the smallest eddies as the thickness of the interface is expected to be of the order of the Kolmogoroff length scale. On the other hand, the delay time must of necessity also be much smaller than the average duration of a burst. For the present work, the hold time over which $(\partial(uv)/\partial t)^2$ was averaged was $\frac{2}{3}$ ms. This corresponds to only two sampling time intervals (one time interval being taken equal to the inverse of the

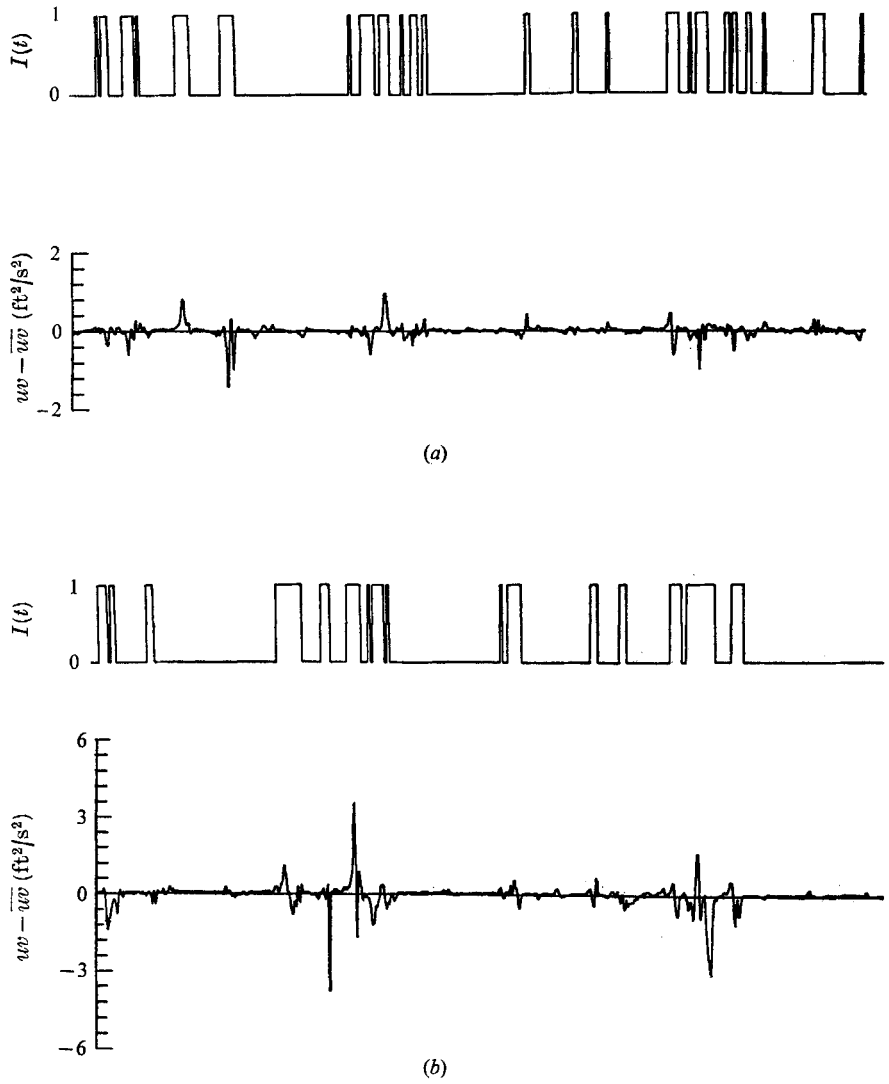

FIGURE 2. Simultaneous uv and $I(t)$ signals for $T_H = 0{\cdot}3\ \overline{(\partial(uv)/\partial t)^2}$. The length of record shown is $\frac{1}{3}$ s. (*a*) Smooth wall. (*b*) Rough wall.

sampling frequency) but remains appreciable compared with an average burst duration of about 2·50 ms (see table 1). Figure 1 shows the variation of $\gamma(\gamma = \bar{I})$ and of the bursting frequency f with T_H, the discriminator setting expressed as a percentage of $\overline{(\partial(uv)/\partial t)^2}$. There is clearly no region on the curve where γ (or f) is independent of T_H, and one has to rely almost entirely on visual observation of simultaneous traces of the uv or $(\partial(uv)/\partial t)^2$ signal and the corresponding $I(t)$ signal. A comparison of these signals was facilitated by computer-plotted traces such as those shown in figure 2. The value of T_H used for figure 2 was

$$0{\cdot}3\overline{(\partial(uv)/\partial t)^2},$$

the value used for all the results of §§4–7. Although the intermittency functions of figure 2 are in general satisfactory there is still some doubt as to whether the brief downward jumps of $I(t)$ from one to zero are to be treated as spurious. There is also doubt as to whether some of the short and relatively low amplitude bursts should have been registered by $I(t)$.

3. Definitions

Measurements are presented here of both zone averages and ensemble averages of instantaneous velocity and Reynolds shear stress fluctuations. The zone average is obtained when the flow property is sampled and averaged only throughout either the turbulent ($I = 1$) or non-turbulent ($I = 0$) zones of the flow. As only the fluctuating components of the velocity signals were recorded on digital tape, the zone and ensemble averages presented in the following sections will refer to only the fluctuating component of velocity. With the instantaneous longitudinal velocity given by $U = \overline{U} + u$ ($\overline{U}$ being the mean velocity) the turbulent- and irrotational-zone averages of u will be denoted by $\overline{u}_t$ and $\overline{u}_p$ respectively, where

$$\overline{u}_t = \overline{Iu}/\overline{I}, \quad \overline{u}_p = \overline{(1-I)u}/\overline{1-I}.$$

It should be noted that the subscripts t and p strictly refer to the overbar and indicate that the averaging is to be carried out over only the turbulent or the irrotational regions of the flow. The quantities $\overline{u}_t$ and $\overline{u}_p$ satisfy the relation $\gamma\overline{u}_t + (1-\gamma)\overline{u}_p = 0$ as $\overline{u} = 0$ by definition. When the quantity of interest is the zone average of the intensity of the fluctuations it is more convenient to look at the departure of u relative to either $\overline{u}_t$ or $\overline{u}_p$. The turbulent-zone average of the intensity of fluctuation of u is then $\overline{(u-\overline{u}_t)_t^2}$ and satisfies the relation

$$\overline{u^2} = \overline{(u-\overline{u}_t)_t^2} + \overline{(1-\gamma)\,(u-\overline{u}_p)_p^2} + \gamma(1-\gamma)\,(\overline{u}_t - \overline{u}_p)^2.$$

The ensemble averages of u are denoted by either $\langle u_t \rangle$ or $\langle u_p \rangle$. $\langle u_t \rangle$ is obtained by first sampling u in a turbulent burst for a given value of t/T, where t is the time measured since the beginning of the burst and T is the total duration of that burst. For a given t/T value, the averaging is then carried out over a number of bursts. Perhaps the most meaningful definition of an ensemble-averaged turbulence intensity is, for the u-component intensity say, $\langle (u - \langle u_t \rangle)_t^2 \rangle$, where the fluctuations are measured relative to the ensemble average $\langle u_t \rangle$.

Another type of average which has been used is the point average (see Kovasznay *et al.* 1970; Kaplan & Laufer 1969) at the front or back of a burst, the sample being taken only at the start (leading edge) or end (trailing edge) of a burst. It is clear that the ensemble average is in fact a point average and the ensemble average distribution within a burst or irrotational patch has to be bounded by the leading- and trailing-edge point averages. As the accuracy of the ensemble or point averages is poorer than that for the zone averages, the ensemble averages presented here were in fact obtained over a relatively small time interval (10 % of T) before being averaged over a number of bursts or irrotational patches. The

mathematical definitions of u_{pf} and u_{pb}, the point velocities of u at the front and back of a burst respectively, are given by

$$u_{pf} = \overline{uP_f}/\overline{P_f}, \quad u_{pb} = \overline{uP_b}/\overline{P_b},$$

where P_f and P_b are the pulse trains corresponding to either the leading edge or trailing edge of the interface. The trains are represented by

$$2P_f = \dot{I}(t) + |\dot{I}(t)|, \quad 2P_b = -\dot{I}(t) + |\dot{I}(t)|,$$

where the dot denotes differentiation with respect to time.

4. Ensemble averages of velocity fluctuations

The ensemble averages $\langle u_t \rangle$, $\langle u_p \rangle$, $\langle v_t \rangle$ and $\langle v_p \rangle$ are shown in figures 3(*a*) and (*b*) (smooth wall) and figures 4(*a*) and (*b*) (rough wall). The position $t/T = 0$ in the figures refers to the downstream or earlier time for both the turbulent and irrotational regions. The distribution of $\langle u_t \rangle$ for the smooth wall is roughly symmetrical with respect to $t/T = 0{\cdot}5$ and is qualitatively similar to the rough-wall distribution. It should be noted that bursts or irrotational zones of duration greater than about 23 ms and less than about 1·6 ms were excluded from the analysis leading to the results of figures 3 and 4.†

Figure 3(*a*) shows that $\langle u_p \rangle$‡ is effectively uniformly distributed in the smooth-wall layer whilst the rough-wall distribution of $\langle u_p \rangle$ (figure 4(*a*)) shows a slight increase near $t/T = 0{\cdot}5$.

The present $\langle u_p \rangle$ distributions are different from those reported in Antonia & Bradshaw (1971) for a mixing layer and a boundary layer at positions in the flows where $\gamma \simeq 0{\cdot}5$. The latter distributions showed a small but definite increase between the end of one burst and the start of the next one, this acceleration being presumably supported by pressure forces.

The values of $\overline{u}_t$ and $\overline{u}_p$§ (see table 1) are, as expected, respectively negative and positive in agreement with the notion of low velocity large-scale bursts entraining faster moving fluid from outside the interface. The present value of $|\overline{u}_t - \overline{u}_p|/U_1$ on the smooth wall is 1·9 %, in good agreement with the value of 2 % found by Kovasznay *et al.* (1970) at an equivalent y/δ position. The rough-wall value of $|\overline{u}_t - \overline{u}_p|/U_1$ is, however, 3·5 % but when the friction velocity U_τ ($U_\tau = \tau_w^{\frac{1}{2}}$, τ_w being the kinematic wall shear stress) is used to normalize the velocity difference $|\overline{u}_t - \overline{u}_p|$ the rough-wall value of 0·54 is in somewhat closer

† The probability of finding bursts of duration greater than 23 ms is extremely small (see figures 5 and 6). Although the frequency of occurrence of bursts of duration less than 1·6 ms is relatively high, there is a possibility that some of these bursts are spurious.

‡ It should be kept in mind that although the irrotational averages are presented in figures 3 and 4 on the same time scale as the turbulent averages, the average duration $\overline{T}_p$ of an irrotational zone is roughly six times larger than the average burst duration $\overline{T}_t$ (see table 1).

§ Note that the zone averages $\overline{u}_t$, $\overline{u}_p$, etc., are obtained for *all* bursts that occur for the length of record examined. This means that the average values under the ensemble average curves of figures 3 and 4 need not be exactly identical to the zone averages for the quantity examined.

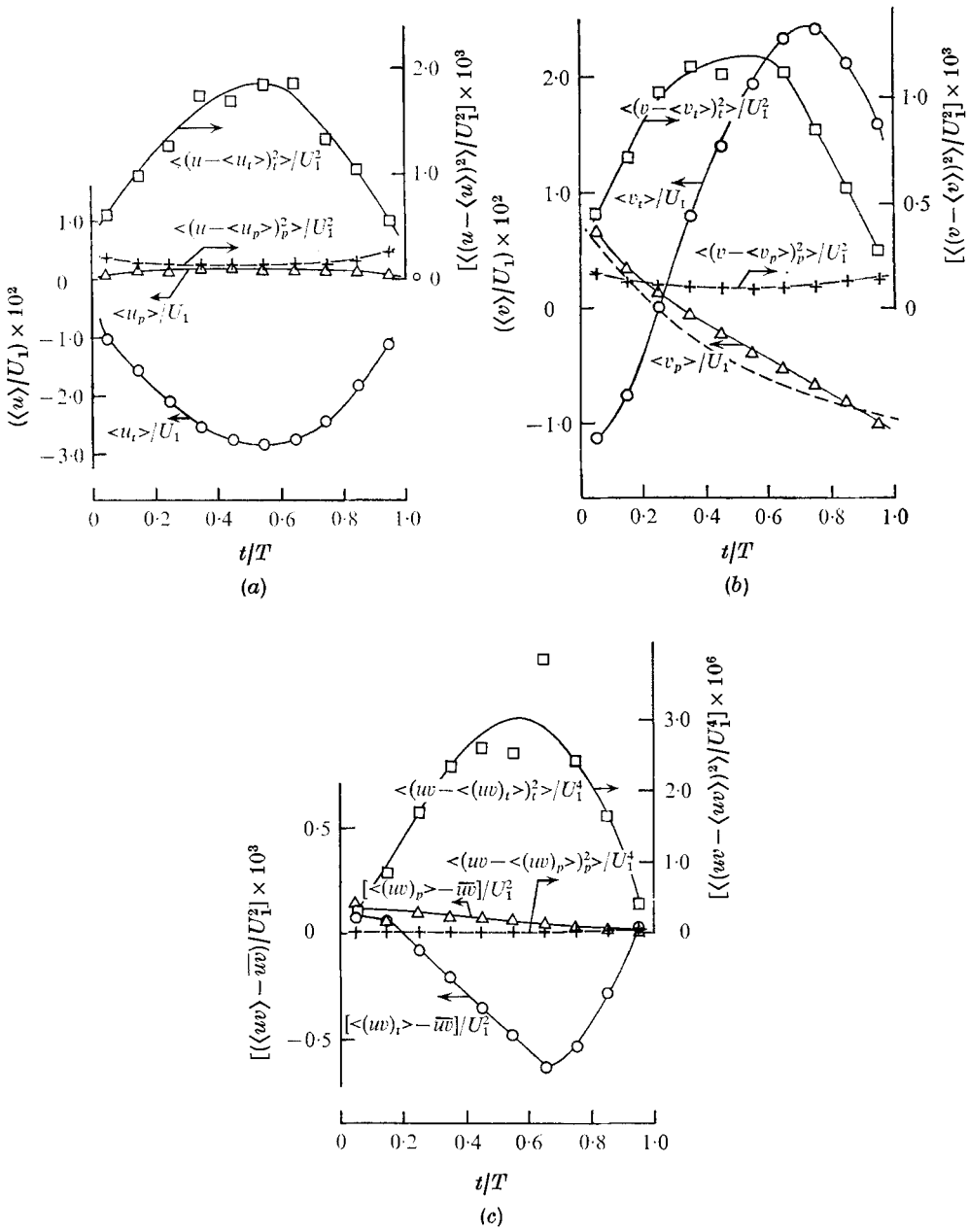

FIGURE 3. Ensemble averages of velocity and Reynolds shear stress fluctuations on smooth wall. (*a*) u fluctuations: ○, $\langle u_t\rangle U_1$; □, $\langle(u-\langle u_t\rangle)_t^2\rangle/U_1^2$; △, $\langle u_p\rangle/U_1$; +, $\langle(u-\langle u_p\rangle)_p^2\rangle/U_1^2$, (*b*) v fluctuations: ○, $\langle v_t\rangle/U_1$; □, $\langle(v-\langle v_t\rangle)_t^2\rangle/U_1^2$; △, $\langle v_p\rangle/U_1$; +, $\langle(v-\langle v_p\rangle)_p^2\rangle/U_1^2$; – – – –, inferred from Kovasznay *et al.* (1970). (*c*) uv fluctuations: ○, $(\langle(uv)_t\rangle-\overline{uv})/U_1^2$; □, $\langle(uv-\langle(uv)_t\rangle)_t^2\rangle/U_1^4$; △, $(\langle(uv)_p\rangle-\overline{uv})/U_1^2$; +, $\langle(uv-\langle(uv)_p\rangle)_p^2\rangle/U_1^4$.

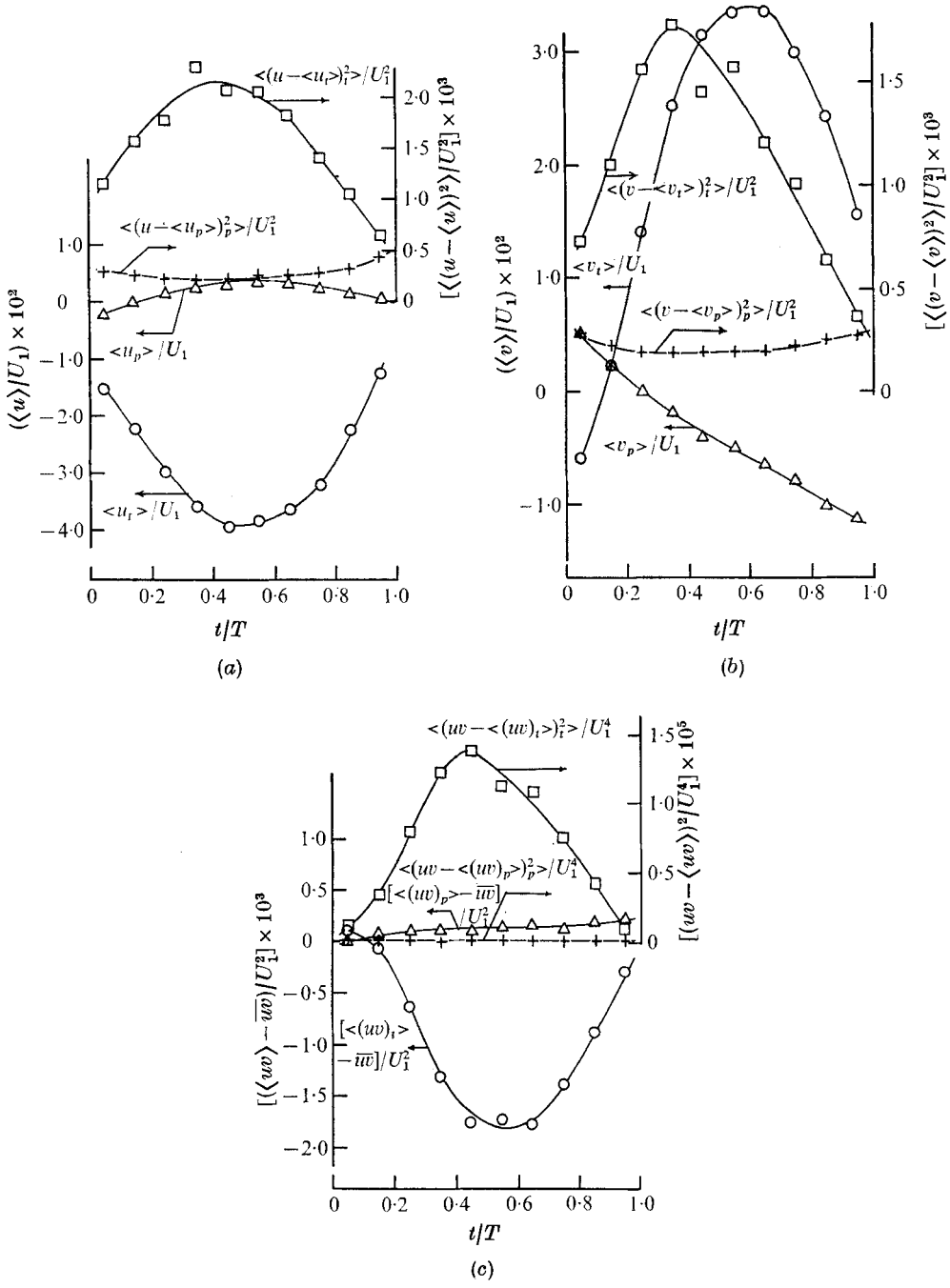

FIGURE 4. Ensemble averages of velocity and Reynolds shear stress fluctuations on rough wall. (*a*) *u* fluctuations, (*b*) *v* fluctuations, (*c*) *uv* fluctuations. Symbols same as for figure 3.

agreement with the smooth-wall value of 0·45.† The difference between $\overline{u}_t$ and $\overline{u}_p$ is given by

$$|\overline{u}_t - \overline{u}_p| = \frac{|\overline{Iu}|}{\gamma} + \frac{|\overline{Iu}|}{(1-\gamma)} = \frac{|\overline{Iu}|}{\gamma(1-\gamma)}.$$

The maximum value of $|\overline{Iu}|$ cannot be greater than $[\overline{(I-\gamma)^2}\,\overline{u^2}]^{\frac{1}{2}}$ or

$$[\gamma(1-\gamma)]^{\frac{1}{2}}(\overline{u^2})^{\frac{1}{2}}.$$

The maximum value of $|\overline{u}_t - \overline{u}_p|$ is therefore given by $(\overline{u^2})^{\frac{1}{2}}/[\gamma(1-\gamma)]^{\frac{1}{2}}$. For the smooth-wall layer, this is equivalent to a maximum value for $|\overline{u}_t - \overline{u}_p|/U_1$ of 5 % and to 6·8 % on the rough wall. If one makes the rather poor assumption that $\overline{u^2} = \gamma\overline{u_t^2}$ then the above maximum value of $|\overline{u}_t - \overline{u}_p|$ reduces to $(\overline{u_t^2})^{\frac{1}{2}}/(1-\gamma)^{\frac{1}{2}}$, and clearly this maximum would be expected in the fully turbulent region of the flow where $\gamma \simeq 1$. This is in agreement with the experimental results of Kovasznay *et al.*, which show that $|\overline{u}_t - \overline{u}_p|$ increases monotonically with increasing γ.

Unlike the distribution of $\langle u_t \rangle$, the shape of $\langle v_t \rangle$ is clearly not symmetrical within a burst. The positive value of $\langle v_t \rangle$ at the upstream end of the burst and the negative value at the downstream end are in agreement with the notion of the outer irrotational flow riding over the turbulent bulges. The maximum value of $\langle v_t \rangle$ is significantly larger for the rough-wall than for the smooth-wall bursts. The distribution of $\langle v_p \rangle$ shows an almost linear decrease between the end of one burst and the start of the next burst. This distribution is essentially the same for the smooth- and rough-wall layers. It should be noted here that the present distributions of $\langle v_t \rangle$ are essentially in agreement with the information inferred from the point-averaged normal-velocity data of Kovasznay *et al.* taken (relative to various positions of the interface) at small values of γ. As γ increases however, the normal velocity becomes negative on the back of the bursts (this actually occurs at $\gamma \simeq 0{\cdot}6$) whilst $\langle v_t \rangle$ still remains negative on the front of the burst. By assuming that the shape of the interface is symmetrical with respect to $t/T = 0{\cdot}5$ in the irrotational flow, a distribution of $\langle v_p \rangle$ was inferred from the point-averaged data of Kovasznay *et al.* at $y/\delta = 0{\cdot}95$. This distribution is shown in figure 3(*b*) and is in reasonable agreement with the present results. The ratio $|\overline{v}_t - \overline{v}_p|/U_1$ is equal to 0·011 on the smooth wall compared with 0·021 on the rough wall. These values are approximately 50 % of the corresponding values obtained for

$$|\overline{u}_t - \overline{u}_p|/U_1.$$

The point-averaged longitudinal velocities at the front and back of a burst, u_{pf} and u_{pb} respectively, were found to be essentially equal on the rough wall. For the smooth wall u_{pf} was slightly greater than u_{pb}, the difference representing only $0{\cdot}001U_1$. The normal velocity v_{pb} is, however, definitely larger than v_{pf}, the difference being $0{\cdot}015U_1$ for the smooth wall and $0{\cdot}010U_1$ for the rough wall. The present difference between u_{pf} and u_{pb} on the smooth wall is essentially in

† Comparison of the smooth-wall and rough-wall results of table 1 suggests that the residual differences when the velocities (or the stresses) are normalized with U_τ (or U_τ^2) may be almost wholly attributable to the difference in y/δ and the consequent rather large difference in γ.

agreement with the results of Kaplan & Laufer (1969). The slightly higher velocity at the leading edge of the burst is probably consistent with the notion that the fronts of the bulges appear to be on average steeper than the backs, a view that is confirmed by observations of smoke-filled boundary layers (see for example Fiedler & Head 1966). Kovasznay *et al.* (1970) find that u_{pf} is less than u_{pb}, a result which appears to be in conflict with their measurements of interface convection velocity (inferred from space–time correlations of the pulse trains P_f and P_b), which show that at $y/\delta = 1{\cdot}0$ the convection velocity at the front is larger than that at the back by almost $0{\cdot}05\,U_1$. This rather large value is however, as Kovasznay *et al.* point out, probably due to the growth of the boundary layer.

5. Reynolds shear stress fluctuations

The ensemble-averaged distributions of the Reynolds shear stress fluctuations are presented in figures 3(*c*) and 4(*c*) in the form $\langle (uv-\overline{uv})_t \rangle$, where $\overline{uv}$ is the conventionally averaged Reynolds shear stress. There is a small region near the front of the burst where $\langle (uv)_t \rangle$ is positive, a consequence of both $\langle u_t \rangle$ and $\langle v_t \rangle$ being negative in this region. The maximum value of $\langle (uv)_t \rangle$ on the smooth wall represents about 41 % of the wall shear stress whilst, for the rough wall, the maximum is approximately 45 % of the wall shear stress. These results together with the values of $(\overline{uv})_t$ shown in table 1 suggest that the shear stress remains significant within the turbulent bursts even though $\overline{uv}$ is practically negligible at this value of y/δ. Although the irrotational-zone average of the shear stress is expected to be zero (this is experimentally confirmed by the present small values of $(\overline{uv})_p$), there is no reason why the ensemble average $\langle (uv)_p \rangle$ should also be zero everywhere.

The intensity of the shear stress fluctuations relative to the ensemble-averaged distribution is given by $\langle (uv-\langle uv \rangle)^2 \rangle$. Within the turbulent bursts, this distribution has a maximum near $t/T = 0{\cdot}5$ and falls rapidly towards the edges of the burst in much the same way as the distributions of $\langle (u-\langle u_t \rangle)_t^2 \rangle$ and $\langle (v-\langle v_t \rangle)_t^2 \rangle$. The distribution of $\langle (uv-\langle (uv)_p \rangle)_p^2 \rangle$ is, however, virtually negligible whilst there are still considerable u and v fluctuations in the irrotational zones. In the case of the rough-wall layer, the ratio $\overline{(uv-(\overline{uv})_t)_t^2}/\overline{(uv-(\overline{uv})_p)_p^2}$ is equal to 164 compared with values of 10 and 7·8 for $\overline{(u-\overline{u}_t)_t^2}/\overline{(u-\overline{u}_p)_p^2}$ and $\overline{(v-\overline{v}_t)_t^2}/\overline{(v-\overline{v}_p)_p^2}$ respectively. This provides some justification for our choice of the uv signal in generating the intermittency function. The r.m.s. value of the shear stress fluctuations relative to the turbulent-zone average is $(\overline{(uv-(\overline{uv})_t)_t^2})^{\frac{1}{2}}$†. When this is normalized by the local turbulent shear stress $(\overline{uv})_t$, the ratio is equal to 4·20 on the smooth and 2·90 on the rough wall. The corresponding values for the conventional shear stress fluctuations $(\overline{(uv-\overline{uv})^2})^{\frac{1}{2}}/(-\overline{uv})$ are 5·77 and 10·05 (see Antonia 1971). In the fully turbulent ($\gamma \simeq 1$) part of the flow, this ratio has approximate values of 3·0 (smooth wall) and 3·5 (rough wall). The actual level of the turbulent shear stress fluctuations as given by $(\overline{(uv-(\overline{uv})_t)_t^2})^{\frac{1}{2}}/\tau_w$ has values of 0·68 (smooth wall) and 0·77 (rough wall) for the present results as compared with a value of approximately

† This may also be regarded as a measure of the range of strengths of the bursts.

2·0 for both the smooth- and the rough-wall boundary layers in the non-intermittent region of the flow. These previous results indicate that, although the level of shear stress fluctuation in the turbulent part of the flow decreases with decreasing γ, the decrease is significantly slower than that of the shear stress averaged within the turbulent billows.

Townsend (1956, p. 145) has indicated that the intermittency factor γ would be indirectly obtained from measurements of the flatness factor of a quantity M since

$$\gamma = \frac{\overline{M_t^4}}{\overline{M_t^2}^2} \Big/ \frac{\overline{M^4}}{\overline{M^2}^2},$$

and if the assumption is made that the turbulent-zone averaged quantities are homogeneous with the turbulent fluid, the above reduces to

$$\gamma = \left(\frac{\overline{M^4}}{\overline{M^2}^2}\right)_{\gamma=1} \Big/ \frac{\overline{M^4}}{\overline{M^2}^2}. \tag{1}$$

Apart from the assumption of homogeneity, the above relation requires that $\overline{M_t^2} = \overline{M^2}/\gamma$, i.e. that $\overline{M_p^2}$ is small compared with $\overline{M_t^2}$. The Reynolds shear stress fluctuations within the irrotational flow are neglibibly small and the flatness factor of $M(= uv - \overline{uv})$ within the turbulent fluid

$$\overline{(uv-\overline{uv})_t^4}/\overline{(uv-\overline{uv})_t^2}^2$$

is equal to 21·9 (smooth wall) and 21·1 (rough wall). These values are, as expected, smaller than the values of 96·6 (smooth wall) and 127 (rough wall) for the conventional flatness factor of $uv - \overline{uv}$ (strictly, this is a hyperflatness factor as it is an eighth-order moment involving fourth-order powers of u and v). They are, however, significantly larger than the value of 9, which corresponds to the flatness factor of the product of uncorrelated Gaussian variables (see Antonia & Luxton 1971*b*). The values of γ derived from the above information are 0·22 (smooth wall) and 0·16 (rough wall), which are, not surprisingly, in good agreement with the value inferred directly from the intermittency function. On the other hand, the use of the flatness factors of the turbulent u and v fluctuations leads to much higher and incorrect values for γ. The assumption that the distribution of any quantity within the turbulent fluid remains homogeneous is clearly not satisfactory and, even in the case of uv, the flatness factor of $uv - \overline{uv}$ in the inner layer is approximately 6 for both smooth- and rough-wall layers. The use of this in (1) would lead to values of γ much lower than the experimental results. The above discussion indicates that relation (1) is unlikely to be satisfactory at least near the edges of an intermittent flow. Wygnanski & Fiedler (1969) also found that in the outer region of a round jet the intermittency derived from the flatness factor of u is significantly higher than that obtained by the counting method. Klebanoff (1955) found, however, that the value of γ was adequately given by the flatness factor of u, at least for values of y/δ up to 0·9.

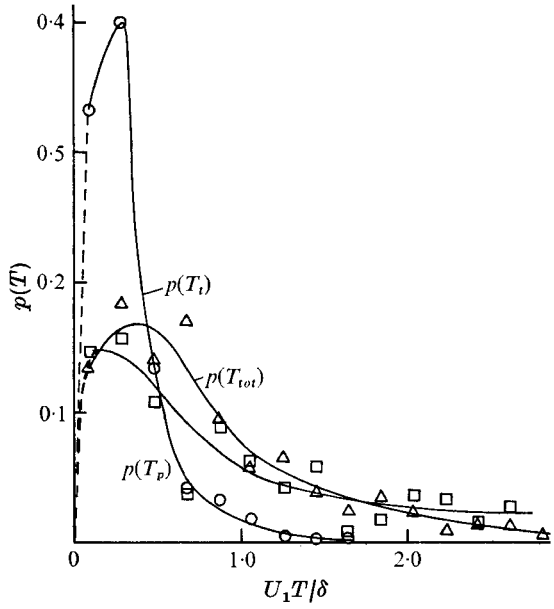

FIGURE 5. Probability density of lengths of turbulent bursts and irrotational patches on smooth wall. ○, $p(T_t)$; □, $p(T_p)$; △, $p(T_{tot})$.

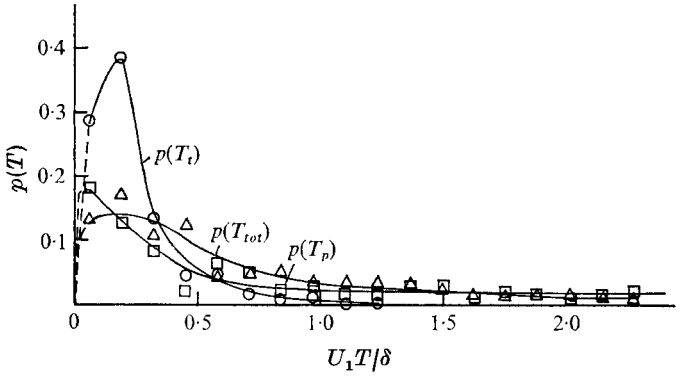

FIGURE 6. Probability density of lengths of turbulent bursts and irrotational patches on rough wall. ○, $p(T_t)$; □, $p(T_p)$; △, $p(T_{tot})$.

6. Probability distributions

The probability densities of T_t, the duration of a turbulent burst, T_p, the duration of an irrotational patch and of T_{tot}, the time interval between two successive bursts, are shown in figures 5 and 6. The distributions of $p(T_t)$ and $p(T_p)$ are essentially in qualitative agreement with the boundary-layer results of Corrsin & Kistler (1955) at $\gamma = 0{\cdot}25$. Although the present results were obtained for a much longer length of record than that used by Corrsin & Kistler, appreciable scatter in the data is still evident particlarly for $p(T_p)$ and $p(T_{tot})$. For very small values of T, Corrsin & Kistler showed, by assuming that the random interface

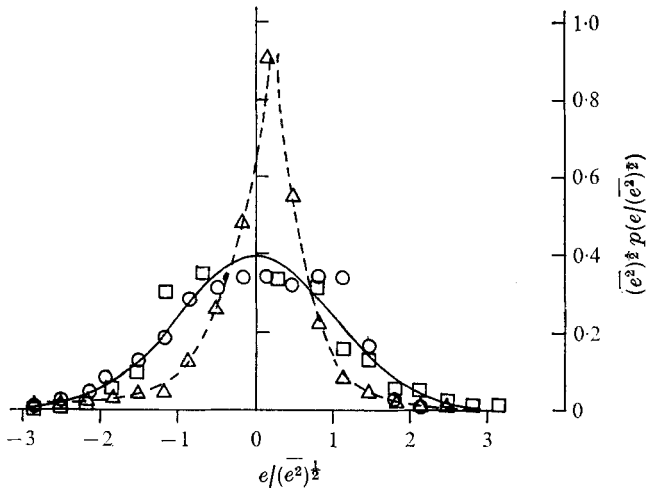

FIGURE 7. Probability density of u, v and uv within the turbulent bursts on smooth wall. ○, $u-\overline{u}_t$; □, $v-\overline{v}_t$; △, $uv-(\overline{uv}_t)$.

position is differentiable, that $p(T_t)$ and $p(T_p)$ must increase linearly away from zero. For values of T greater than $\overline{T}_t$, or $\overline{T}_p$, the distributions of $p(T_t)$, and $p(T_p)$, represent reasonable approximations to exponential distributions, suggesting that, for this range of T at least, the frequency of occurrence of a given interface position follows a Poisson distribution. The present values of $(U_1\overline{T}_t/\delta)$ and $(U_1\overline{T}_{tot}/\delta)$ on the smooth wall are in good agreement with those obtained by Kovasznay *et al.* (1970) at the same y/δ position (note that in their figure 3 $L\gamma/2\delta$ should be replaced by $L\gamma/4\delta$). Although the present value of $U_1\overline{T}_{tot}/\delta$ is also in reasonable agreement with the $R_{22}\,(r,0,0)$ correlation half-wavelength obtained by Grant (1958) at $y/\delta \simeq 0{\cdot}5$, it is somewhat surprising, in view of the large spread of T_{tot} (figure 5), that any periodicity is visible in the correlation. If σ represents the standard deviation of the interface relative to its mean position then an indication of the 'waviness' of the interface may be given by $2\sigma/\overline{T}_{tot}$. Assuming that $\sigma \simeq 0{\cdot}14$ for both the smooth and rough walls (see Klebanoff 1955; Corrsin & Kistler 1955) then $2\sigma/\overline{T}_{tot}$ is 0·16 for the smooth wall and 0·15 for the rough wall.

Figure 7 shows the probability densities of u, v and uv within the turbulent bursts in the smooth-wall boundary layer. The results are presented in the non-dimensional form $e/(\overline{e^2})^{\frac{1}{2}}$ *vs.* $(\overline{e^2})^{\frac{1}{2}}\,p(e/(\overline{e^2})^{\frac{1}{2}})$ such that $\int_{-\infty}^{\infty} p(e)\,de = 1$. Here e stands for either $u-\overline{u}_t$, $v-\overline{v}_t$ or $uv-(\overline{uv})_t$, all of these quantities being taken in only the turbulent part of the flow. The densities of $(u-\overline{u}_t)$ and $(v-\overline{v}_t)$ are seen to lie close to but not exactly on the normal distribution. The flatness factors of $(u-\overline{u}_t)$ and $(v-\overline{v}_t)$ are 2·86 and 2·95 respectively, compared with values of 9·82 and 7·82 for the conventional flatness factors for the u and v signal. The probability density of $uv-(\overline{uv})_t$ is negatively skewed with a flatness factor of 21, which is much larger than the value of 13·0 obtained in the fully turbulent inner layer.

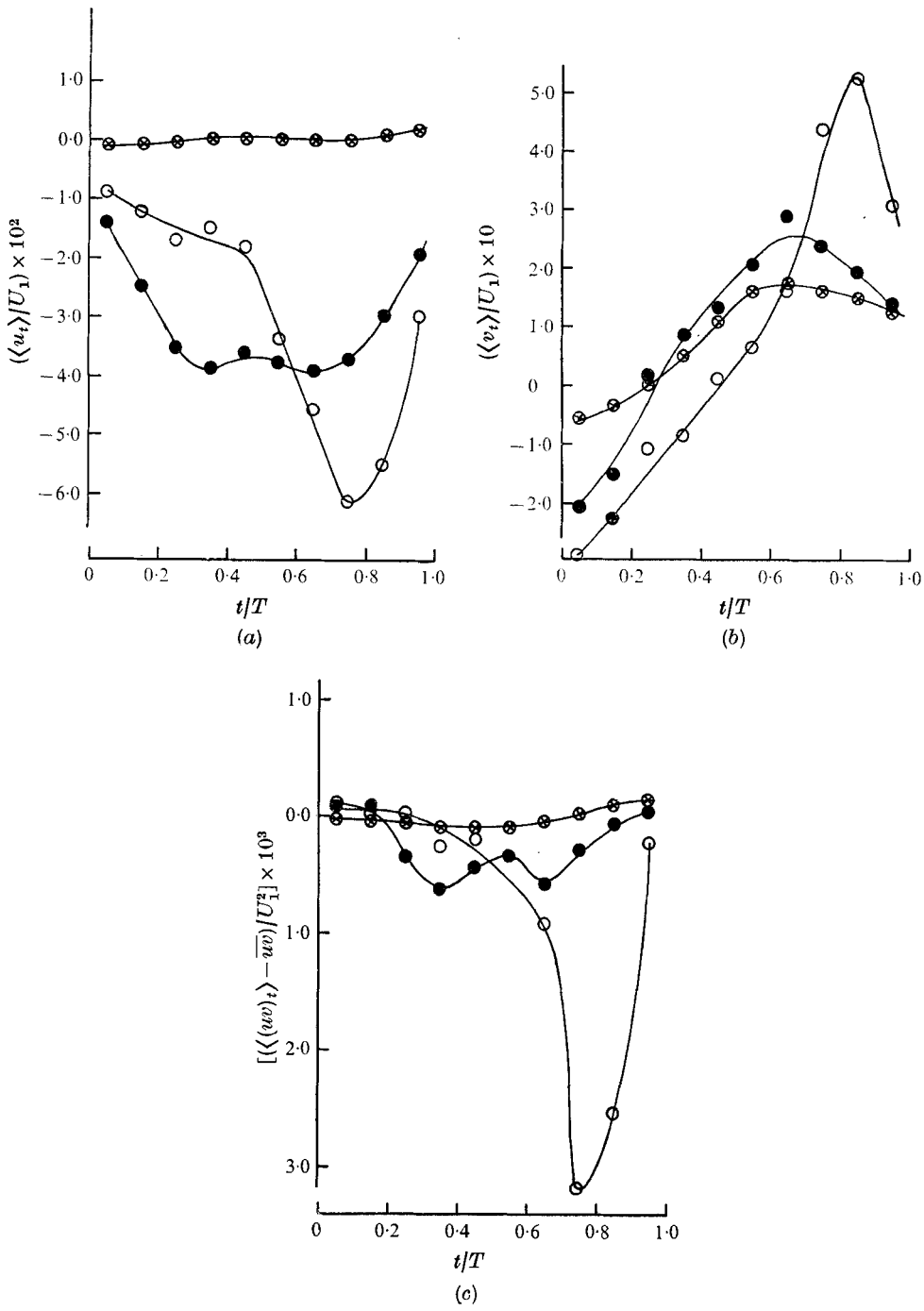

FIGURE 8. Effect of burst duration on ensemble averages of u, v and uv fluctuations in smooth-wall boundary layer. ⊗, $0{\cdot}72 < T/\overline{T}_t < 1{\cdot}44$, number of bursts counted = 88; ●, $1{\cdot}44 < T/\overline{T}_t < 2{\cdot}88$, number of bursts counted = 34; ○, $2{\cdot}88 < T/\overline{T}_t < 4{\cdot}32$, number of bursts counted = 10.

(*a*) $\langle u_t\rangle/U_1$; (*b*) $\langle v_t\rangle/U_1$; (*c*) $(\langle(uv)_t\rangle-\overline{uv})/U_1^2$.

7. Properties of bursts of different durations

Distributions of $\langle u_t \rangle$, $\langle v_t \rangle$ and $\langle (uv)_t \rangle$ in the smooth-wall boundary layer are shown in figure 8 for three different ranges of burst duration. The use of burst duration was adopted, mainly for convenience, as a first attempt to indicate the 'age' of a burst at the time of measurement but there may be more suitable choices. One possibility is the use of the velocity jump (either for the longitudinal or normal velocity or for both) relative to the irrotational field velocity as an indication of the activity of strength of the burst under examination. Another possibility may be the use of the intensity of fluctuation within a particular burst, but, as Townsend (1956) has pointed out, the difficulty is that the intensity of a fluid parcel which has been moved across the flow by the large eddy notion may not be much different from that of similar fluid parcels at different positions at the time of observation.

The results of figure 8 reveal the following features.

(i) The shortest and also more probable (see figure 5) bursts considered ($0{\cdot}72 < T/\overline{T}_t < 1{\cdot}44$) have a longitudinal velocity which is approximately equal to the local mean velocity $\overline{U}$ and contribute negligibly to the local shear stress $\overline{uv}$. The normal velocity of the bursts, however, remains significant compared with the average normal mean velocity $\overline{V}$.

(ii) For the longest duration and relatively less probable bursts considered the distributions of $\langle u_t \rangle$ and $\langle (uv)_t \rangle$ become strongly asymmetric with respect to $t/T = 0{\cdot}5$, the minimum values occurring near the upstream end of the burst. The average longitudinal velocity in these bursts is smaller than $\overline{U}$ while the peak in the $\langle v_t \rangle$ distribution is significantly larger than $\overline{V}$. The maximum value of $\langle (uv)_t \rangle$ in figure 8(*c*) is almost 70 % higher than the local wall shear stress. In Antonia & Bradshaw (1971), it was found that the turbulence associated with the longer bursts had the very nearly Gaussian characteristics of inner-layer turbulence. It appears likely from the above information that the bursts examined here probably originate from the inner region of the boundary layer and arrive in the outer regions of the flow with a significant normal velocity. It should be noted however that only a few bursts were examined here and little weight should be given to the quantitative results of figure 8. For the $3\frac{1}{2}$ s record examined only 10 bursts were obtained in the range $2{\cdot}88 < T/\overline{T}_t < 4{\cdot}32$.

8. Conclusions and discussion

Results of the ensemble averages of the u, v and uv fluctuations within the turbulent regions near the outer intermittent edge of a turbulent boundary layer have revealed that the structure of the bursts is essentially the same for both the smooth- and rough-wall conditions examined. The magnitudes of the rough-wall averages are higher, however, than those for the smooth wall, the discrepancy being apparently explained by the larger surface shear stress in the case of the rough wall. One interesting feature of the $\langle uv \rangle$ distributions is that the maximum value obtained within the turbulent bursts represents approximately 45 % of the wall shear stress. This result provides support for the idea that the large eddy

motion is strong, the strength of the large eddies being closely related to τ_w. The distributions of the intensities of the fluctuations of u, v and uv relative to their respective ensemble averages are roughly symmetrical with respect to $t/T = 0{\cdot}5$. The shapes of $\langle u_t \rangle$ and $\langle v_t \rangle$ are in agreement with the picture of Kovasznay *et al.* (1970) of the irrotational flow passing over the eddies as over a wavy wall. The level of the shear stress fluctuations with respect to $\langle (uv)_t \rangle$ remains high, the average value of the r.m.s. value of these fluctuations representing approximately 70 % of the wall shear stress.

The properties of the turbulence within the bursts are closely similar but not quite identical to the nearly Gaussian properties of inner-layer turbulence. Although the scarcity of the number of bursts may affect the quantitative interpretation of the results of §7, it is evident that (i) bursts of fairly short duration retain an appreciable distribution of $\langle v_t \rangle$ but practically negligible $\langle u_t \rangle$ and $\langle (uv)_t \rangle$ distributions and (ii) bursts of longer duration carry with them a larger mean velocity or momentum defect and an appreciable shear stress distribution.

From the experimental data presented here there seems to be little doubt that the large-scale bursts observed near the outer region of the boundary layer originate from or at least extend through to the inner region of the flow. There has been some speculation however as to whether some of the properties of the large-scale bursts can be directly identified with those of the rather smaller scale and probably more frequent 'bursts' or eruptions observed by Kline *et al.* (1967) in the close vicinity of a smooth surface. The viscous sublayer as such does not exist on the rough wall and the flow visualization experiments of Liu, Line & Johnston (1966) on a rough surface identical to that used here have clearly established the absence of the 'bursts' observed near a smooth wall. These 'bursts' incidentally lose their identity very shortly after their appearance but, as Kovasznay (1970) speculates, it seems likely that they give rise to not easily discernable intermediate size bursts which may in turn be responsible for the large-scale structure in the outer region of the layer. Although the small-scale eruptions are absent on the rough wall, the information about the wall shear stress appears to have been efficiently transferred to the outer-layer structure, the transfer presumably arising through the large diffusion of turbulent energy away from the rough surface. The above considerations can only suggest that the features associated with the small-scale 'bursts' at the outer edge of the viscous sublayer need not be directly responsible for the observed features of the large-scale motion near the outer edge of the boundary layer.

The author is indebted to Mr P. Bradshaw for his suggestions during the course of this work. The work described in this paper represents part of a programme of research supported by The Australian Research Grants Committee, The Australian Institute of Nuclear Science and Engineering and The Commonwealth Scientific and Industrial Research Organization.

REFERENCES

ANTONIA, R. A. 1971 *Dept. Mech. Engng, University of Sydney, Charles Kolling Res. Lab. Tech. Note*, F-29.

ANTONIA, R. A. & BRADSHAW, P. 1971 *Imperial College Aero. Rep.* no. 71–04.

ANTONIA, R. A. & LUXTON, R. E. 1971*a* *J. Fluid Mech.* **48**, 721.

ANTONIA, R. A. & LUXTON, R. E. 1971*b* *Dept. Mech. Engng, University of Sydney, Charles Kolling Res. Lab. Tech. Note*, F-31.

CORRSIN, S. & KISTLER, A. L. 1955 *N.A.C.A. Rep.* no. 1244.

FIEDLER, H. & HEAD, M. R. 1966 *J. Fluid Mech.* **25**, 719.

FRASER, D. 1969 *Dept. Mech. Engng, University of Sydney, Charles Kolling Res. Lab. Tech. Note*, F-9.

GRANT, H. L. 1958 *J. Fluid Mech.* **4**, 149.

IMAKI, K. 1968 *Bull. Inst. Space Aeronaut. Sci., University of Tokyo*, **4**, 448 (in Japanese only).

KAPLAN, R. E. & LAUFER, J. 1969 *Proceedings of the 12th International Congress on Applied Mechanics*, p. 236. Springer.

KIM, H. T., KLINE, S. J. & REYNOLDS, W. C. 1968 *Stanford University, Dept. Mech. Engng Rep.* MD-20.

KLEBANOFF, P. S. 1955 *N.A.C.A. Rep.* no. 1247.

KLINE, S. J., REYNOLDS, W. C., SCHRAUB, F. A. & RUNSTADLER, P. W. 1967 *J. Fluid Mech.* **30**, 741.

KOVASZNAY, L. S. G. 1970 *Ann. Rev. Fluid Mech.* **2**, 95.

KOVASZNAY, L. S. G., KIBENS, V. & BLACKWELDER, R. F. 1970 *J. Fluid Mech.* **41**, 283.

LIU, C. K., LINE, S. J. & JOHNSTON, J. P. 1966 *Stanford University, Dept. Mech. Engng Rep.* MD-15.

ROTTA, J. C. 1956 *Ing. Arch.* **24**, 258.

TOWNSEND, A. A. 1949 *Aust. J. Sci. Res.* **2**, 451.

TOWNSEND, A. A. 1956 *The Structure of Turbulent Shear Flow.* Cambridge University Press.

WYGNANSKI, I. 1971 *Israel J. Tech.* **9**, 105.

WYGNANSKI, I. & FIEDLER, H. E. 1969 *J. Fluid Mech.* **38**, 577.

WYGNANSKI, I. & FIEDLER, H. E. 1970 *J. Fluid Mech.* **41**, 327.